



Synthesis of Magnetite (Fe_3O_4) Nanoparticles from Iron sands by Co-precipitation-Ultrasonic Irradiation Methods

R. Rahmawati^{1,3}, A. Taufiq⁴, S. Sunaryono⁴, A. Fuad⁴, B. Yulianto^{1,2*},
S. Suyatman¹, D. Kurniadi¹

¹Engineering Physics Department, Faculty of Industrial Technology, Institut Teknologi Bandung, Bandung Indonesia 40132

²Research Center of Nanosciences and Nanotechnology, Institut Teknologi Bandung, Bandung Indonesia 40132

³Department of Physics, Faculty of Sains and Technology, UIN Sunan Kalijaga Yogyakarta, Indonesia 55281

⁴Department of Physics, Faculty of Mathematics and Natural Sciences, Universitas Negeri Malang (State University of Malang), Jl. Semarang 5 Malang, Indonesia 65145

Received 31 Jan 2017,
Revised 29 May 2017,
Accepted 31 May 2017

Keywords

- ✓ Co-precipitation
- ✓ Iron sands
- ✓ Magnetite
- ✓ Superparamagnetic behavior
- ✓ Ultrasonic-irradiation

brian@tf.itb.ac.id,

Phone: (+62) 22 2504424
ext 132

Abstract

Magnetite (Fe_3O_4) nanoparticles have been synthesized from iron sands with both co-precipitation and co-precipitation—ultrasonic irradiation methods. X-ray diffraction (XRD) patterns showed that Fe_3O_4 samples generated by these two synthesis methods are in a single phase with a cubic spinel structure. This research investigates the influence of ultrasonic irradiation in the synthesis process including size, morphology, composition and magnetic properties. The morphology of Fe_3O_4 was characterized by a transmission electron microscopy (TEM) instrument. The TEM image of Fe_3O_4 synthesized using the ultrasonic irradiation method showed a reduction of the agglomeration of the Fe_3O_4 particles. Moreover, the TEM images also showed that the primary particles of Fe_3O_4 prepared by the co-precipitation method tend to agglomerate as the particles cluster, with the particle size ranging from 9 to 33 nm. Meanwhile, Fe_3O_4 synthesized using the ultrasonic irradiation method tends to construct a primary particle sized about 25 to 37 nm. The magnetic properties that were characterized by vibrating sample magnetometer (VSM) measurement showed that Fe_3O_4 exhibited superparamagnetic behavior at room temperature.

1. Introduction

Recently, Fe_3O_4 nanoparticles has gained enthusiastic attention from many researchers due to their unique properties in nanoscale, such as a large surface area, high surface energy, low toxicity, good biocompatibility, superparamagnetic behavior, high absorption, and transfer electrons [1-3]. In recent trend on sensor development, the nanostructure have been attracted many researchers to prepare the metal oxide nanostructure because that kind of materials have several advantages including large surface area so that the materials will be more sensitive and easy for absorption and desorption of the targeted sensors object [4-7]. Relating to biomedical applications, Fe_3O_4 nanoparticles have been commonly used for magnetic scaffolds [8], gene delivery [9,10], cell therapy [11], magnetic resonance imaging [12,13], cell labelling [14], hyperthermia [15,16], and drug delivery [17,18].

Several methods have been developed by researchers to obtain Fe_3O_4 nanoparticles, including hydrothermal [19], co-precipitation [20], sonochemical [21], solvothermal [22], microemulsion [23], and gamma irradiation [24]. However, co-precipitation has become the preferred method in preparing Fe_3O_4 nanoparticles because of its many advantages, including short time reaction, the ability to use water as a solvent, cost effectiveness, simplicity, high productivity, and its low-temperature process [25-26]. On the other hand, the Fe_3O_4 nanoparticles are very easy to agglomerate because of their large surface-volume ratio and high surface energy. Therefore, the combination of methods—adding ultrasonic irradiation during the co-precipitation process—becomes one alternative method to control the size and shape of Fe_3O_4 nanoparticles.

The synthesis of Fe₃O₄ nanoparticles using ultrasonic irradiation at room temperature with the main commercial precursors has been conducted by many researchers [25, 29-30]. However, the synthesis of Fe₃O₄ nanoparticles by heating the sample using a local natural iron sands as a main precursor has not been reported yet. As reported by other researchers and our group that the iron sands can be synthesized become Fe₃O₄ nanoparticles, due to the naturally high iron (Fe) content in iron sands, depending on the locations in which they were collected [26-30, 34-35]. Therefore, this paper reports on the use of irradiation of ultrasonic waves for preparing magnetite nanoparticles from iron sands in combination with the co-precipitation method. Finally, the crystal structure, size of particle, morphology, and magnetic properties of the samples will be discussed.

2. Materials and Methods

2.1 Sample preparation

The main precursors in this experiment are iron sands from the southern coast of Indonesia, 12 M HCl (99%, Sigma Aldrich), 3.5 M NaOH (99%, Sigma Aldrich), and distilled water. All reagents were used without further purification. The synthesis methods of Fe₃O₄ are divided into two parts: the first synthesis uses only co-precipitation, and the second synthesis uses co-precipitation with ultrasonic irradiation. Iron sands were first extracted by using a permanent magnet. The resulting extractions are then dissolved with the HCl at 80°C with a constant stirrer of 700 rpm. The solution is then filtered and slowly etched with NaOH while being heated to a temperature of 70°C to obtain black precipitate. The detail of synthesizing Fe₃O₄ particles from iron sands using the coprecipitation method is adapted from our previous work [31,32]. Moreover, the Fe₃O₄ synthesized by ultrasonic irradiation follows the same procedure as the previous method, except that ultrasonic waves irradiation (Phywe Generator, 200 KHz/10 W) was used while dropping the NaOH into the solution for two hours to obtain a black precipitate. The resulting precipitate was then washed repeatedly with distilled water to remove residual material.

2.2 Characterization of Fe₃O₄ nanoparticles

2.2.1 XRD analysis

The Fe₃O₄ particles were characterized by X-ray diffractometer (PHILIPS PW 1800, Cu K α radiation λ = 1.5406 Å at 40 kV and 40 mA) to investigate the phases and crystal structures.

2.2.2 XRF analysis

The elemental compositions of the samples were investigated with X-ray fluorescence (PANalytical MiniPal 4).

2.2.3 TEM analysis

The transmission electron microscopy (JEOL JEM1400) was used to determine the size and morphology of the particles. The sample was dissolved by ethanol and sonicated for 15 minutes, after that dropped on carbon grid and dried at room temperature.

2.2.4 VSM analysis

The vibrating sample magnetometer (Oxford VSM1.2H) was used to verify the magnetic properties of the Fe₃O₄ particles. The magnetic properties were analyzed based on the hysteresis curves to determine the coercivity field, remanent magnetization, and saturation magnetization. The measurement was conducted at room temperature with a magnetic field ranging from -1 to 1 Tesla.

3. Result and discussion

The pattern of X-ray measurement has been matched in the ICSD database with the model No. 82237. Based on the XRD results, the iron sands samples extracted with the permanent magnets have a Fe content of more than 77%, with the balance being other elements. This result is in accordance with the XRF results as shown in Table (1). Analysis of the XRD patterns indicates that the Fe₃O₄ extracted by permanent magnet still has micrometer-sized particles. The XRD spectra of resulting samples synthesized by the co-precipitation method and ultrasonic irradiation showed no other phase besides the phase of Fe₃O₄. It can therefore be concluded that the Fe₃O₄ resulting from the synthesis is pure single phase. According to the ICSD database model No. 82237, both of the nano Fe₃O₄ samples synthesized by co-precipitation and co-precipitation-ultrasonic irradiation have a cubic

spinel structure with lattice parameters $a = b = c = 8.387 \text{ \AA}$. These results indicate that the use of ultrasonic radiation does not affect the structure of Fe_3O_4 .

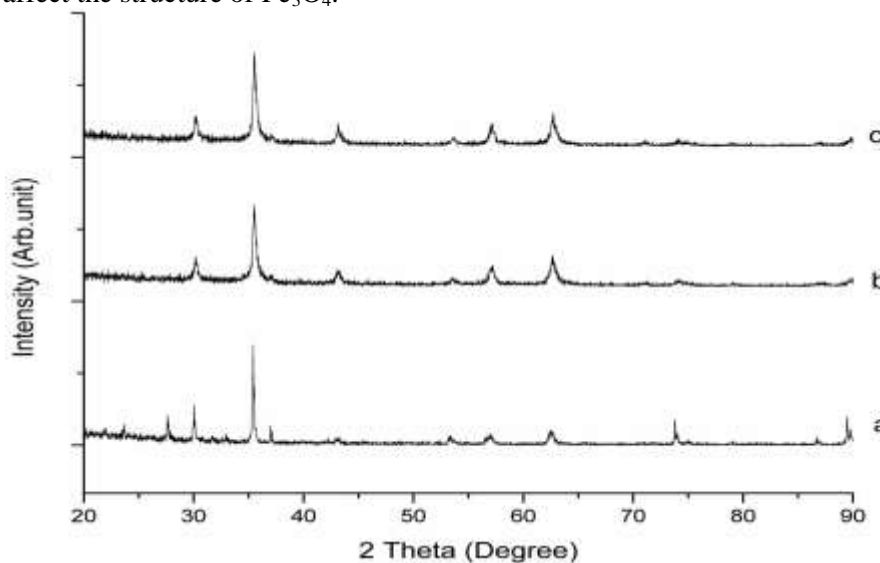


Figure 1: XRD spectra of Fe_3O_4 from iron sands extracted with a permanent magnet (a), Fe_3O_4 nanoparticles synthesized by the co-precipitation method (b), and Fe_3O_4 nanoparticles synthesized by co-precipitation with ultrasonic irradiation (c).

The characterizations for composition of samples using XRF are shown in Table (1). From Table (1), it is clear that using a permanent magnet as a tool for the extraction of iron sands is effective in raising the Fe element content from 44.3% to 77.4%. Moreover, the synthesis process using the co-precipitation method is able to increase the Fe content from about 12.00% to 89.76%, although the samples still contained impurities such as Ti (around 5%) and other elements making up less than 1%. The Fe element increases when the samples are synthesized using ultrasonic irradiation compared with the co-precipitation method amounted to 90.35%, although impurities such as Ti (more than 5%) and other elements making up less than 1% still exist. Yang et al revealed that the use of ultrasound for the synthesis of Fe_3O_4 is able to increase the amount of Fe^{3+} ions from Fe^{2+} that are oxidized [33]. According to the XRD spectra as shown in Figure (1), the ultrasonic irradiation does not change the structure of Fe_3O_4 . Therefore, it can be said that the oxidation process occurs only on the surface of the particle. The more appropriate analysis of the XRD record explains that the Fe_3O_4 synthesized using the co-precipitation method and ultrasonic irradiation is of single phase. It could be that the impurity components (Ti, Eu, Ca, and so on) are atoms that make up the individual form. According to Mashuri et al [26], the impurity of atoms can be partially substituted in the atoms of $\text{Fe}^{2+}/\text{Fe}^{3+}$ in the structure ferrites of spinel.

Table 1: Elemental composition of the synthesized Fe_3O_4 as determined by X-ray fluorescence (XRF)

Sample	Element Content (% weight)															
	Fe	Al	Si	P	K	Ca	Ti	V	Cr	Mn	Ni	Cu	Zn	Br	Eu	Re
Iron sands*	44.3	5	20	0.53	1.91	20.2	3	0.21	0.1	1.1	1.79	0.21	0.04	0.55	0.48	0.44
Iron sands**	77.4	4	5.5	0.4	0.44	2.32	6.16	0.46	0.11	0.61	1.12	0.11	0.11	0.23	0.62	0.2
Fe_3O_4 ***	89.76	-	-	0.1	-	0.73	5.44	0.41	0.11	0.58	-	-	0.08	0.35	0.89	0.3
Fe_3O_4 ****	90.35	-	-	0.2	-	0.67	5.18	0.36	0.22	0.56	-	-	0.08	0.34	0.9	0.3

*Iron sands ; ** Iron sands were extracted by permanent magnet; *** Fe_3O_4 were synthesized by co-precipitation;**** Fe_3O_4 were synthesized by ultrasonic irradiation

Figure (2) shows the morphology of the Fe_3O_4 particles using TEM measurement for iron sandss, Fe_3O_4 synthesized by the co-precipitation method, and Fe_3O_4 synthesized by ultrasonic irradiation. Based on the TEM record, it is confirmed that the result is in accordance with the XRD measurements of Fe_3O_4 iron sands extracted with a permanent magnet where the particle size is about a micrometer with unclear morphology. Meanwhile, there is a fairly large agglomeration, and the particles tend to form the clusters on Fe_3O_4 synthesized by the co-precipitation method, as shown in Figure (2b). Moreover, based on deeper analysis of the

TEM results, it is apparent that at the inside of the agglomeration, a group of Fe_3O_4 particles with diameters between 9 and 33 nm are shown by white circles. This phenomenon showed that the synthesis of Fe_3O_4 using the co-precipitation process performed at pH 9 and a temperature of 70°C is not enough to break the agglomeration that occurs in Fe_3O_4 particles. This analysis is also supported by the condition of Fe_3O_4 particles, which are very prone to agglomerate due to the strong magnetic forces among their particles. Conversely, a very striking morphological difference of Fe_3O_4 resulted from the synthesis process using ultrasonic irradiation, as shown in Fig. 3(c), where the agglomeration of particles breaks up and tends to form primary particles with spherical shapes in diameters of about 25–37 nm. Jamie et al [34] reported that when the ultrasonic waves were irradiated in the medium, there is a high-pressure difference that passes through the particles and causes high shear stress on them. Therefore, cavitation and shock waves occurring in the slurry can accelerate solid particles moving at high speed, and the collisions between these particles will produce significant changes in the morphology of the particle surface.

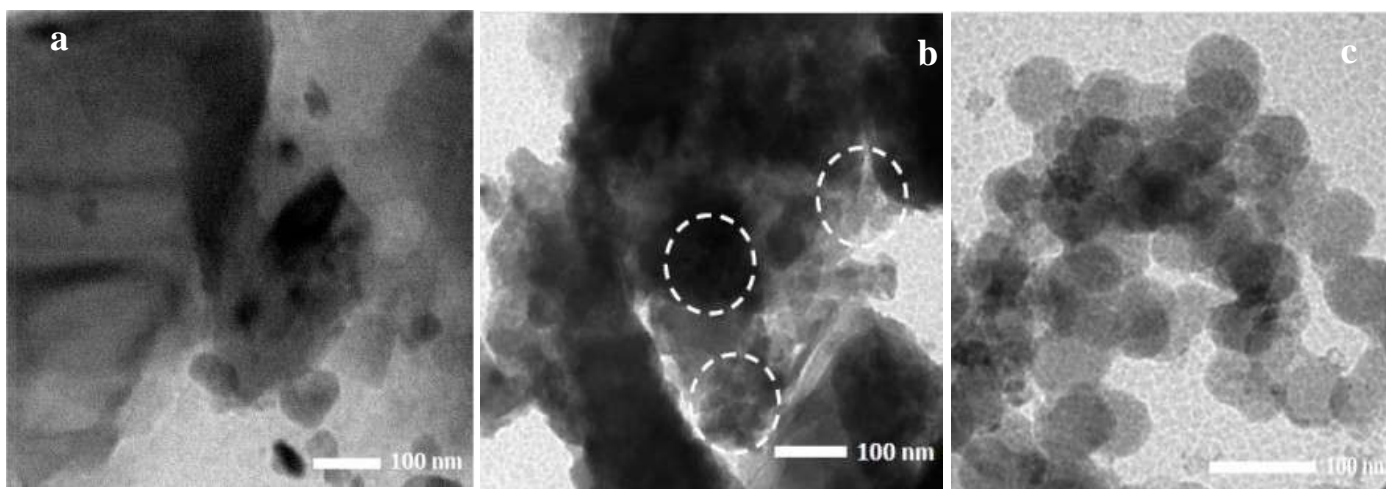


Figure 2: TEM image of (a) iron sands extracted by permanent magnet, (b) Fe_3O_4 synthesized by co-precipitation, and (c) Fe_3O_4 synthesized by co-precipitation with the ultrasonic irradiation method. The circle marks indicate the agglomeration of Fe_3O_4 .

Magnetic properties identification of Fe_3O_4 was conducted using the hysteresis curve analysis between Magnetization (M) and applied field (H) which resulting from the VSM test at room temperature, as shown in Figure (3). The amount of such magnetic coercivity (H_c), remanent magnetization (M_r), and saturation magnetization (M_s) becomes the basis for the analysis of magnetic properties of the Fe_3O_4 sample, as shown in Table (2).

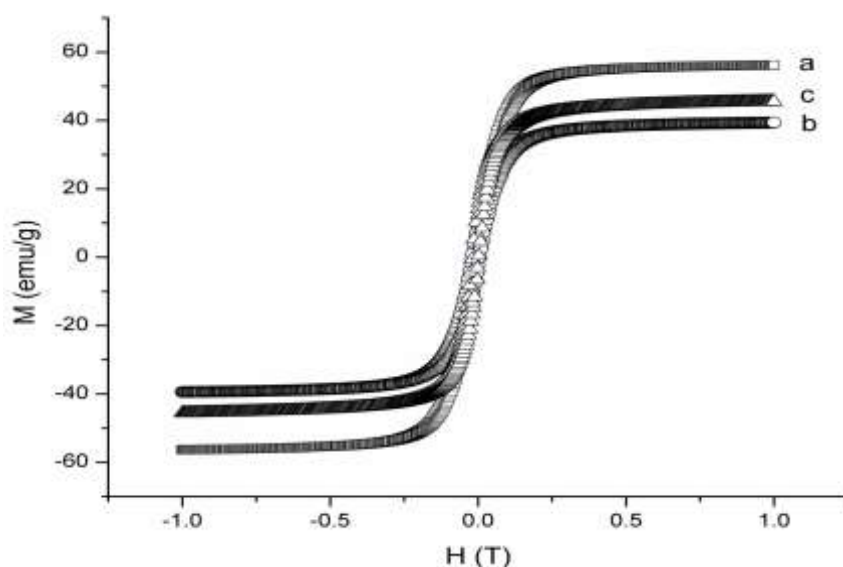


Figure 3: VSM result of (a) iron sands extracted by magnet permanent, (b) Fe_3O_4 synthesized by co-precipitation and (c) Fe_3O_4 synthesized by co-precipitation with ultrasonic irradiation

Table 2. Magnetic properties of Fe₃O₄

No	Sample	Ms (emu/g)	Mr (emu/g)	Hc (H)
1	Iron sands	56,200	3,693	4,479
2	Co-precipitation with ultrasonic irradiation	45,500	5,850	0,014
3	Co-precipitation	39,281	6,518	0,006

It can be seen that the biggest saturation magnetization belongs to the Fe₃O₄ from the iron sands extracted by permanent magnets in the amount of 56.2 emu/g. This value is less than the saturation magnetization of Fe₃O₄ bulk, which is between 88 and 90 emu/g [35,36]. This low saturation magnetization value of the samples is due to the many impurities in the iron sands. Meanwhile, the saturation magnetization of Fe₃O₄ synthesized using the co-precipitation method has a smaller value than that synthesized using ultrasonic irradiation, which are 39.281 emu/g and 45.5 emu/g, respectively. This phenomenon is according to the TEM results that the Fe₃O₄ particle synthesized using the co-precipitation method is smaller than that irradiated with the ultrasound. It is found that the saturation magnetization of Fe₃O₄ is strongly influenced by the particle size, where the smaller the particle size of Fe₃O₄, the lower the saturation magnetization of Fe₃O₄ [34]. According to domain theory stating that as the particle size gets smaller, the number of domains becomes fewer and tend to form a single domain, this condition will decrease the amount of the magnetic moment and result in a reduction of the saturation magnetization of Fe₃O₄. Table (2) shows that the Fe₃O₄ samples generated from this study tend to have superparamagnetic behavior at room temperature, which is indicated by the Hc value that is close to zero. Based on their magnetic properties especially from Ms values, the Fe₃O₄ nanoparticles resulted from this research exhibit promising potential for bio application [37-38].

Conclusion

In Summary, this research has successfully synthesized the Fe₃O₄ nanoparticles from iron sands by using the co-precipitation method and the co-precipitation with ultrasonic irradiation method. The Fe₃O₄ synthesized by the co-precipitation method and the co-precipitation with ultrasonic irradiation method have particle sizes of 9–33 nm and 25–37 nm, respectively. Moreover, this research revealed that ultrasonic irradiation is able to reduce agglomeration that occurs during the synthesis process, so that the morphology of the particles tends to be clear and almost homogeneous. The Fe₃O₄ nanoparticles have superparamagnetic behavior at room temperature, making them more suitable for potential usage in bioapplications including biosensor, drug delivery and hyperthermia.

Acknowledgments –This research was partially supported by Scholarship dissertation of Lembaga Pengelola Dana Pendidikan (LPDP) and "Hibah Kompetensi" research grant of Ditlitabmas, Ditjen DIKTI, 2016. Authors would like to thank for Central Laboratory for Minerals and Advanced Materials Faculty of Mathematics and Natural Sciences Universitas Negeri Malang (State University of Malang) for the characterization of XRD and XRF.

References

1. J P. Cheng, R. Ma, Shi D., F. Liu, X.B. Zhang, *J. Ultrason Sonochem.* 18 (2011) 1038-1042
2. G. S. Cao, P. Wang, X. Li, Y. Yuewang, G. Wang, J. Li, *Bull. Mater. Sci.* 38 (2015) 163-167
3. S.F. Chin, S.C. Pang, C.H. Tan, *J. Mater. Environ. Sci.* 2 (2011) 299-302
4. N.L.W. Septiani, B. Yulianto, *J. Electrochem Soc.* 163 (3) (2016) B97 – B106.
5. B. Yulianto, L. Nulhakim, M.F. Ramadhani, Suyatman, A. Nuruddin, *IEEE Sens. J.* 15 (7) (2015), 4114 – 4120.
6. H. Abderrahim, M. Berrebia, A. Hamou, H. Kherief, Y. Zanoun, K. Zenata. *J. Environ. Sci.* 2 (2011) 94-103.
7. S.S. Ibrahim, *J. Environ. Sci.* 2 (2011) 118-127.
8. N. Bock, A. Riminucci, C. Dionigi, A. Russo, A. Tampieri, E. Landi, V.A. Goranov, M. Marcacci, V. Dediu, *J. Acta Biomater.* 6 (2010) 786-796

9. Y. Chen, G. Lian, C. Liao, W. Wang, L. Zeng, C. Qian, K. Huang, X. Shuai, *Am J Gastroenterol* 48 (2013) 809-821
10. G. Liu, J. Xie, F. Zhang, Z. Wang, K. Luo, L. Zhu, Q. Quan, G. Niu, S. Lee, H. Ai, X. Chen, *J.Small* 7 (2011) 2742-2749
11. S. I. Jenkins, H. H. P. Yiu, M. J. Rosseinsky, D. M. Chari, *Molecular and Cellular Therapies* 2 (2014) 23
12. O. Veisoh, J. W. Gunn, M. Zhang, *J. Adv Drug Deliv Rev.* 62 (2010) 284-304
13. C. Li, T. Chen, I. Ochoy, G. Zhu, E. Yasun, M. You, C. Wu, J. Zheng, E. Song, C. Z. Huang, W. Tan, *J.Adv. Funct. Mater.* 24 (2014) 1772-1780
14. C. Wilhelm, F. Gazeau, *J. Biomaterials.*, 29 (2008) 3161-3174
15. G.V. Fernandez, O. Whear, A. G. Roca1, S. Hussain, J. Timmis, V. Pateland, K. O'Grady, *J. Phys. D: Appl. Phys.*, 46 (2013) 1-6
16. X.L. Liu, H. M. Fan, J. B. Yi, Y. Yang, E. S. G. Choo, J. M. Xue, D. D. Fan, Ding J., *J. Mater. Chem.* 22 (2012) 8235-8244
17. C. Chen, Jiang X., Y.V. Kaneti, A. Yu, *Powder Technol.* 236 (2013) 157-163
18. J. Yue, X. Jiang, Y.V. Kaneti, A. Yu, *J Colloid Interf Sci* 367 (2012) 204-212
19. H. Yan, J. Zhang, C.You, Z. Song, B.Yu, Y. Shen, *J. Mater Chem Phys.* 113 (2009) 46-52
20. F. Chen, S. Xie, J. Zhang, R. Liu, *J. Mater Lett.* 112 (2013) 177-179
21. S. Wu, A. Sun, F. Zhai, J. Wang, W. Xu, Q. Zhang, A. A. Volinsky, *J. Mater Lett.* 65 (2011) 1882-1884
22. C. Li, Y. Wei, A. Liivat, Y. Zhu, J. Zhu, *J. Mater Lett.*107 (2013) 23-26
23. T. Lu, J. Wang, J. Yin, A. Wang, X. Wang, T. Zhang, *J. Colsurfa A: Physicochem. Eng. Aspects.* 436 (2013) 675-683
24. A. Abedini, A. R.Daud, M. A. A.Hamid, N. K. Othman, *J. PLoS ONE.* 9 (2014) 1-8
25. Y. Mizukoshi, T. Shuto, N. Masahashi, S. Tanabe, *J. Ultrason Sonochem.* 16 (2009) 525-531
26. Mashuri M., Triwikantoro T., Yahya E., Darminto D., *Journal of Materials Science and Engineering A I.* 5 (2011) 182-189
27. S. Sunaryono, Taufiq A., Mashuri M., Pratapa S., Zainuri M., Triwikantoro T., Darminto D., *J. Materials Science Forum* 827 (2015) 229-234
28. Y. Dong, Y. Chang, Q. Wang, J. Tong, J. Zhou, *Bull. Mater. Sci.* 39 (2016) 35-39
29. M. N. Islam, L.V. Phong, J. R. Jeong, C. Kim, *J. Thin Solid Films* 519 (2011) 8277-8279
30. J P. Cheng, R.Ma, D. Shi, F. Liu, X.B.Zhang, *J. Ultrason Sonochem.* 18 (2011) 1038-1042
31. A. Taufiq , S. Sunaryono, E. G. R. Putra, A. Okazawa, I. Watanabe, N. Kojima, S. Pratapa, D.Darminto, *J Supercond Nov Magn.* 28 (2015) 2855-2863
32. A. Taufiq, S. Sunaryono, E.G.R. Putra, S. Pratapa, D. Darminto, *J. Materials Science Forum.* 827 (2015) 213-218
33. C. Yang, G. Wang, Z. Lu, J. Sun, J. Zhuang, W. Yang, *J. Mater.Chem.* 15 (2005) 4252-4257
34. M. R. Jamei, M. R. Khosravi, B. Anvaripour, *Asia-Pac. J. Chem. Eng.* 8 (2013) 767-774
35. Z. Huang, F. Tang, *J. Colloid Interface Sci.* 281 (2005) 432-436
36. J. Feng, J. Mao, X.Wen, M. Tu, *J Alloy Compd.* 509 (2011) 9093-9097
37. N. A. Brusentsov, V. V. Gogosov, T. N. Brusentsova, A.V. Sergeev, N. Y. Jurchenko, A. A. Kuznetsov, Kuznetsov O. A., Shumakov L.I., *J Magn Magn Mater* 225 (2011) 113-117
38. M. Anbarasu, M. Anandan, E. Chinnasamy, V. Gopinath, K. Balamurugan, *Spectrochim Acta A* 135 (2015) 536-539

(2018) ; <http://www.jmaterenvirosci.com>